Department of Applied and Social Pharmacy, Medical University of Lublin, Lublin, Poland

The *in vitro* photocytotoxicity of photosensitizer encapsulated by nanovehicles comprising biomimetic phospholipids

J. Sobczyński*, B. Chudzik-Rząd

Received April 8, 2020, accepted July 9, 2021

**Corresponding author: Jan Sobczyński, Department of Applied and Social Pharmacy, Medical University of Lublin, Lublin, 20-903 Lublin, Poland*
jan.sobczynski@umlub.pl

Pharmazie 76: 532-537 (2021) *doi: 10.1691/ph.2021.0047*

Photosensitizers (PSs) for use in antimicrobial photodynamic therapy (aPDT) are often characterized by poor solubility and a tendency to aggregate in aqueous environments. Mixed nanomicellar drug delivery systems based on Pluronics block copolymers and biomimetic phospholipids (Colalipids) may enhance the efficiency of photosensitizers. The aim of the present work was to explore a mixed nano-micellar drug delivery composed of Pluronic P123 and three different biomimetic phospholipids (Colalipids). Interactions between the PSs and P123/Colalipids assemblies were studied at micromolar concentration by means of UV-Vis absorption spectrometry and by photon correlation spectroscopy. The prepared nanocarriers efficiently solubilized model PS precluding its aggregation in aqueous media. P123/Colalipid assemblies formed small, positively charged micelles that efficiently delivered PS to fungal cells leading to cell death following exposure to blue light *in vitro*. It was found that mixed micelles based on short and medium chain phospholipids caused higher fungal cell reduction as compared to their long chain counterpart. The clinically relevant, CA2 strain was more resistant to aPDT *in vitro* treatment, as compared to model ATCC strain. However the treatment with optimized formulation caused 6 log CFU reduction of cell survival in CA2 cultures upon light activation.

1. Introduction

Antimicrobial photodynamic therapy (aPDT), also called photodynamic inactivation of microbial pathogens, is a treatment modality used to eradicate pathogenic microorganisms, *e.g.* Gram-positive and Gram-negative bacteria and fungi (Wainwright 2009). The non-specific mechanism of action, localized approach and aPDT selectivity reduces the number and severity of side effects, as compared to systemic antibiotic treatment and provides a valuable therapeutic opportunity for eradicating antibiotic-resistant strains. The aPDT action requires three crucial elements: oxygen (O_2), a nontoxic dye, called photosensitizer (PS), and harmless low-intensity visible light of an appropriate wavelength (Sobczyński and Polski 2017). The photochemical mechanism of aPDT is based on PS activation by light energy and the resulting production of a highly energized triplet state. Subsequently various radicals and reactive oxygen species are formed, *e.g.* singlet oxygen, $^1O_2$, that damage different microbial cellular structures leading to cell death. Typically, the blue light (λ= 420-490 nm) is employed in aPDT (Takasaki et al. 2009). The efficiency of aPDT treatment relies on several factors associated with its respective components, *i.e.*, the oxygen, light, PS. The higher efficiency can be expected following longer irradiation time and higher photosensitizer dose (Hamblin and Hasan 2004). The efficiency will also differ depending on the pathogen species to be treated, due to the hurdles to the penetration of photosensitizer into microbial cells. Due to differences in outer membrane structure, Gram-negative bacteria are less susceptible to aPDT, as compared to Gram-positive bacteria (Johnson et al. 2014). Fungi present a target even more complex than bacteria, as their cells are surrounded by a rigid cell wall, separated from the cell membrane by a periplasmic space. The cell wall is built of a mixture of saccharides and lipoproteins. In order to anchor it to proteins and lipids within cellular membrane, the PS designed to treat fungi should be slightly hydrophobic (Dai et al. 2012). Clinical aPDT research focuses on treating local, skin, or soft tissue infections, *e.g.*, chronic leg ulcers as well as infected wounds in diabetic patients. Other directions include catheter- and prosthesis-associated infections associated with biofilm formation.

Many photosensitizers employed in aPDT research are porphyrins. The absorption spectrum of most tetraphenyl porphyrin monomeric free bases is characterized by the presence of a single, intense, narrow band at around 400 nm called the Soret band (Gouterman 1978). The changes in the absorption spectra of meso-porphyrins have previously been utilized to assess the presence of different porphyrin species, *i.e.* monomers, dimers and aggregates and to differentiate between acidic and basic form (Lilletvedt et al. 2011a). Moreover, the analysis of the spectra serves to detect the interactions between photosensitizer and drug vehicle on a mechanistic level and determine the impact of pharmaceutical formulation on their photochemical reactivity (Lilletvedt et al. 2011b). Nanoparticulate carriers have been proven effective in delivering small molecules to the microbial targets (Devrim and Bozkim 2017). Various nanocarriers, notably liposomes have been used as photosensitizer delivery agents, as previously reviewed (Ghosh et al. 2019). The small size and resulting large surface area-to-mass ratio are nanoparticles' most significant advantage. It accounts for elevated contact surface, which yields a high internalization rate by cells. A carrier's surface properties, *i.e.*, size, charge, and shape, will determine its behavior in the biological milieu, *i.e.* efficient cell internalization and penetration into biofilm water channels (Beirão et al. 2014). It has previously been demonstrated that the drug delivery nanocarriers based on ethylene oxide and propylene oxide (Pluronics; Fig. 1) may improve the aqueous solubility of PSs, and decrease PS aggregation (Sobczyński et al. 2014),

Abbreviations
aPDT – photodynamic therapy; ATCC – American Type Culture Collection; cmc – critical micelle concentration; FWHM – full width at half maximum; $^1O_2$ – singlet oxygen; PDI – polydispersity index; PS – photosensitizer; THPP – 5,10,15,20-Tetrakis (4-hydroxyphenyl) porphine

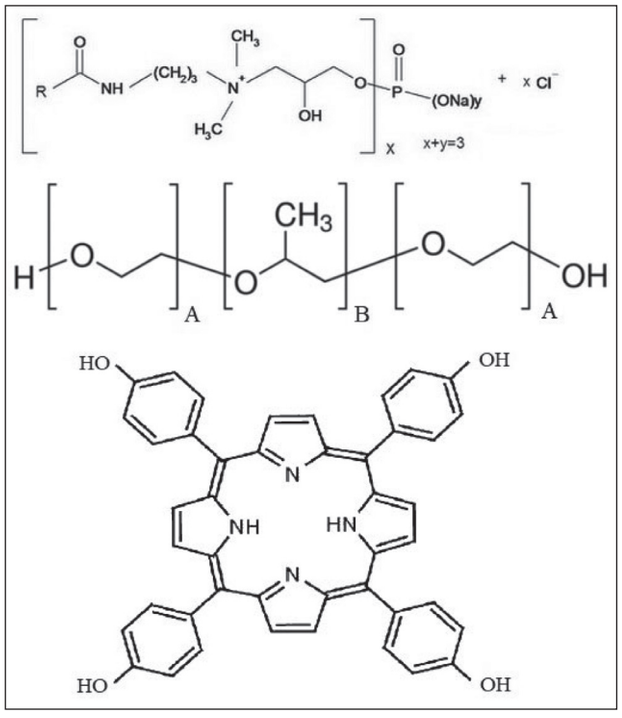

Fig. 1: Structural formula of the Colalipids (top), Pluronic P123 block copolymer (middle) and 5,10,15,20-tetrakis(4-hydroxyphenyl) porphine (THPP; bottom). R – radical denoting coco fatty acids (Colalipid C), myristic acid (Colalipid M) and borage fatty acids (Colalipid BP). A – the average number of ethylene oxide groups (39), the average number of propylene oxide groups (69).

subsequently increasing their photochemical activity. Moreover, PS internalization by cells can be improved, considering a proper selection of the polymer properties.

At present Pluronics are used in many commercial formulations and have been extensively studied for the drug delivery purposes (Batrakova and Kabanov 2018; Pitto-Barry and Barry 2014). The properties of the Pluronic micelles can be modified by addition of another surface active agent, leading to formation of mixed micelles. Mixed micelles are versatile drug delivery carriers, due to multitude of beneficial properties provided by the discrete components (Sobczyński and Chudzik-Rząd 2018). One can construct a binary surfactant system comprising two polymers, where one provides high drug solubilization via hydrophobic interactions, while the other surfactant ensures high binding capacity at the targeted site due to high affinity of the polymer to the targeted biological site (Paszko et al. 2011). Colalipids are PG-Dimonium Chloride Phosphate derivatives of natural fatty acids. They are utilized as multifunctional ingredients in personal care products, *e.g.* creams, lotions, tonics, shower gels, facial washes and other cream-base toiletries as well as hair care products, *e.g.* conditioners, shampoos, hair tonics, hair creams, etc. at concentration levels ranging from 1 to 3%. They display a broad range of functional attributes including gentle cleansing and foaming properties, reduction of irritation caused by the anionic surfactants, high substantivity and long-lasting skin conditioning effect. Moreover, they exhibit a broad spectrum antimicrobial activity towards Gram(+), Gram(-) bacteria and fungi. Importantly, they have been reported as non-irritating and non-cytotoxic (Fost and Yablonski 1997). The antimicrobial potential of these agents may be attributed to the ease of mixing of biomimetic phospholipids with phospholipids naturally occurring within bacterial and fungal cell membranes. Despite their biological activity they have not been used extensively in drug delivery (King et al. 2002; Otto et al. 2010). No reports for using them in antibacterial or antifungal formulations were found.

The aim of current study was to explore new nanocarrier formulations for the *in vitro* photodynamic treatment of *Candida albicans*. Secondly, the goal was to assess the solubilization of model photosensitizer on the molecular level by use of spectroscopic methods. Thirdly, the formulations' morphology was analyzed, including variables important for drug delivery, *i.e.* particle size and z-potential by use of the dynamic light scattering and electrophoretic light scattering, respectively. Finally, the *in vitro* photodynamic efficiency was evaluated in planktonic cultures of two different *C. albicans* strains, including the model strain from ATCC collection as well as a clinically relevant strain.

2. Investigations and results

2.1. Spectral evaluation of PS-nanomicelle interactions

The model photosensitizer used in this study, 5,10,15,20-tetrakis(4-hydroxyphenyl) porphine (THPP), represents the meso-tetrakis phenyl substituted series of porphyrins. The compound comprises a porphine ring, which is substituted at the 5,10,15 and 20 positions with neutral -OH groups (Fig. 1). The Soret band of THPP (417 nm) is broad (FWHM = 51.5 nm) with a small shoulder at 475 nm when the PS is present in pure distilled water (Fig. 2A). Two regions can be distinguished in the curves presented in Fig. 2B. A the P123/Colalipid mixture concentration < 0,00005% no absorptivity increase can be found at the PS's λ_{max}. At higher concentrations, a stepwise growth of Soret band absorptivity is observed. Further, the absorbance increased upon increase of P123/Colalipid assemblies concentration following logarithmic trend. The PS showed slightly higher absorptivity when solubilized by P123/Colalipid BP assemblies, as compared to P123/Colalipid C and P123/Colalipid M formulations. Furthermore, following an increase of P123/Colalipid C concentration the Soret band of THPP gradually became narrow and intense as opposed to flat band observed in aqueous environment. This could be seen as the reduction of full width at half maximum (FWHM) of the Soret band

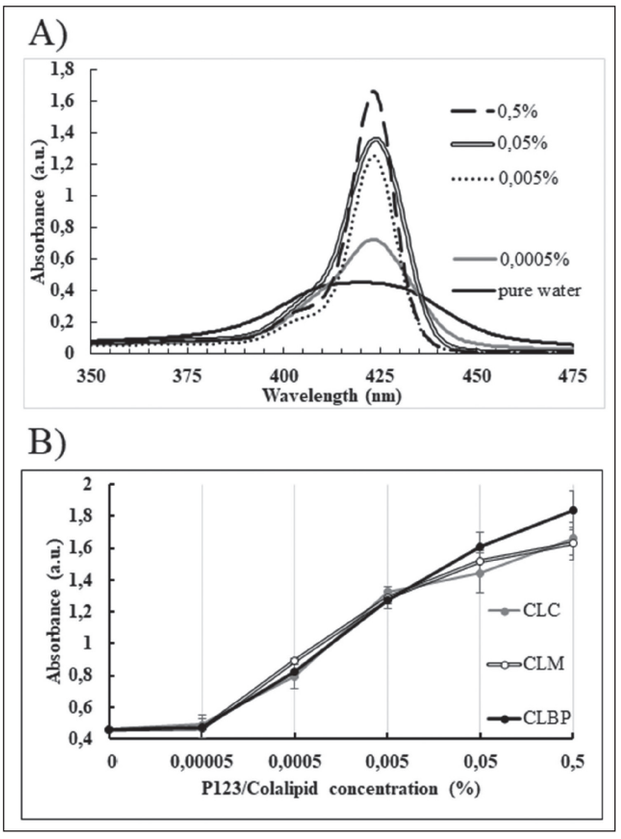

Fig. 2: A) Representative UV-Visible absorption spectra of 5 µM THPP at different P123/Colalipid C concentrations in aqueous solution. B) Absorbance of THPP at the absorption maximum (λ = 417-423,5 nm) as a function of P123/Colalipids concentrations in aqueous solutions containing P123/Colalipid C (CLC), P123/Colalipid M (CLM), P123/Colalipid BP (CLBP). Each point is an average of ≥5 measurements.

from 28 nm at 0,0005% of P123/Colalipid C to 13 nm at 0,5% of P123/Colalipid C. Moreover, the absorption maximum was red-shifted upon addition of P123/Colalipid assemblies from ~417nm to ~423,5nm. The changes of the absorption spectra of two other formulations were similar in respect to the peak width evolution (data not shown).

2.2. Particle characterization

Pluronic P123 is well known to form spherical micelles with well-defined cores > critical micelle concentration (cmc), as also shown by the monodisperse size distribution of 0,5% P123 (Z-average: 22,08±0,47 nm; PDI: 0,09±0,02). Size distribution changes upon addition of Colalipids. A bimodal distribution can be observed for P123-Colalipid assemblies (Fig. 3). Blank P123/Colalipid C formulation exhibits two peaks with maxima at ~7 nm and ~70 nm. Similarly, P123/Colalipid M also shows two peaks with maxima at ~7nm and ~100nm. As for the P123/Colalipid BP two peaks are observed with maxima at ~5 and ~45 nm. The proportion between the two peaks differs for each formulation. For P123/Colalipid BP, the peak at 5 nm is more prominent, as compared to the peak at 45 nm. In P123/Colalipid C formulation the larger peak is more intense, while the two peaks in P123/Colalipid exhibited similar intensity. Following the addition of PS one peak is detected in case of all examined P123/Colalipid formulations. The peaks represent monodisperse distribution with particle ranging from ~2 to ~ 20 nm (Table). Zeta potential differs substantially between formulations ranging from 12.8±1.29 for P123/Colalipid C assemblies to 50.4±2.74 for P123/Colalipid BP formulation.

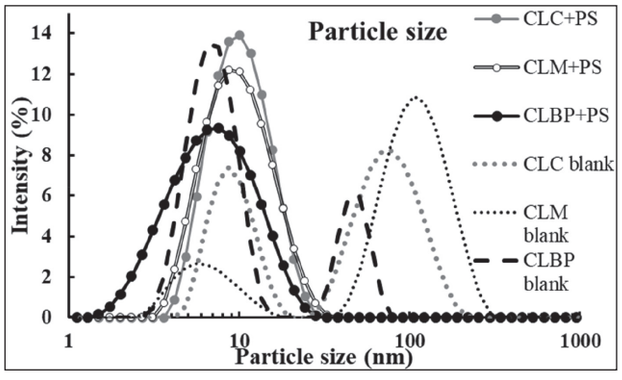

Fig. 3: Representative size distribution by intensity of aqueous solutions of 0,5% P123/Colalipid assemblies (CLC-P123/Colalipid C; CLM-P123/Colalipid M; CLBP – P123/Colalipid BP) in the absence (blank) and presence of 60 μM THPP (PS). The size distribution curves are representative for 5 replicate measurements

Table: Average particle size (Z-average), zeta potential and polidispersity index ±SD (n=5) of P123/Colalipid assemblies containing THPP (5 μM)

Formulation	Particle size (nm)	PDI	Zeta potential (mV)
P123/Colalipid C	9,191±0,045	0,171±0,022	12,8±1,29
P123/Colalipid BP	8,462±0,495	0,109±0,052	50,4±2,74
P123/Colalipid M	8,854±0,061	0,164±0,011	26,2±2,45

2.3. Photobiological experiments

The photobiological experiments were performed in three stages. Firstly, the susceptibility of *C. albicans* planktonic cultures to blank Pluronic P123/Colalipid assemblies was tested in order to determine the non-toxic working range. Secondly the dose escalation studies were performed in regard to both photosensitizer dose and light dose. The delivered blue light (420-450 nm) was specifically chosen to match the absorption spectrum of the selected photosensitizer (the Soret band at 415-435 nm). Finally, the clinical isolates of *C. albicans* cultures were treated using optimized photosensitizer concentration and irradiation time parameters.

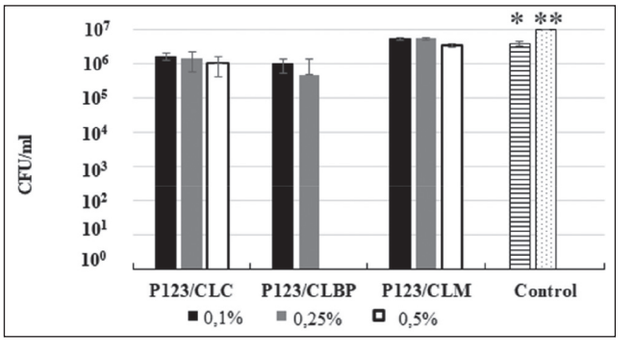

Fig. 4: Cell survival of *C. albicans* cells (ATCC strain) after 60 min incubation with different concentrations of P123/Colalipid C (P123/CLC), P123/Colalipid M (P123/CLM), P123/Colalipid BP (P123/CLBP) formulations in the absence of the light (±SD; n=6). * Control cultures for P123/Colalipid C and P123/Colalipid M experiments; ** Control cultures for P123/Colalipid M experiments.

C. albicans cultures exposed to blank P123/Colalipid C and P123/Colalipid M assemblies for 60 min exhibited negligible reduction in cell survival at concentration up to 0.5%. The P123/Colalipid BP formulation, however eradicated all fungal cells at 0,5% concentration level. Thus, for the latter formulation a working concentration of 0,25% was used. Photocytotoxicity of different THPP doses in the presence of three examined P123/Colalipids assemblies is presented in Fig. 5. *C. albicans* American Type Culture Collection (ATCC) strain cultures exhibited high susceptibility to aPDT treatment. THPP at doses > 20μM were required to eradicate all microbial cells following 20 min irradiation time for P123/Colalipid C and 60 min for P123/Colalipid M formulation. After 30 min of light irradiation, THPP at low doses (*i.e.* 5 and 10 μM) caused 2 log reduction and total eradication when used in P123/Colalipid M and P123/Colalipid C formulations, respectively. The cell survival of *C. albicans* ATCC strain was PS-dose independent and decreased similarly with increasing irradiation times for all examined THPP concentrations.

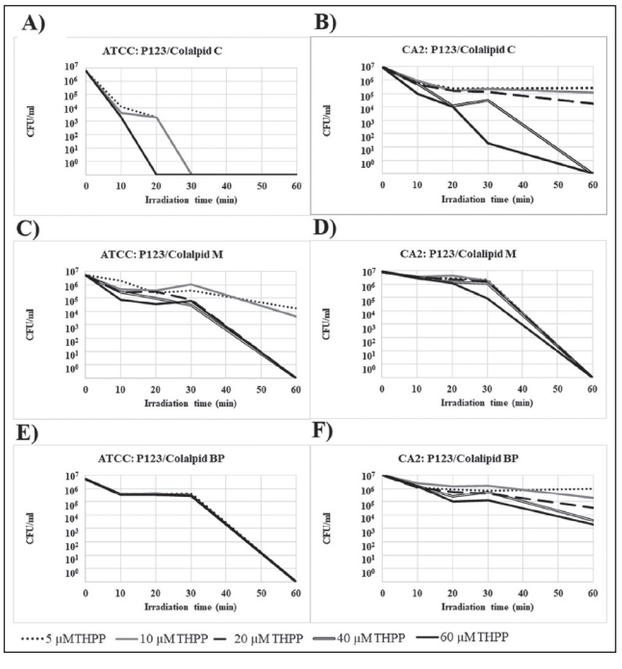

Fig. 5: Cell survival of *C. albicans* cells (model ATCC strain - A, C, E and CA2 strain - B, D, F) after aPDT treatment with 0,5 % P123/Colalipid C (A and B), 0,5 % P123/Colalpid M (C and D), 0,25 % P123/Colalipid C (E and F) formulations containing THPP at different concentration levels. The data points are presented as the mean of one experiment, SE ≤ 20%. The average CFU/ml in control experiments (cultures not exposed to light or formulations) was 4,9 x 10^6 for ATCC cultures (A, C, E) and 9,2 x 10^6 for CA2 cultures (B, D, F).

C. albicans CA2 strain cultures were less prone to aPDT treatment, as compared to ATCC strain. When solubilized by P123/Colalipid C formulation, only 40 and 60 μM THPP concentrations were able to completely eradicate *C. albicans* cultures following 60 min irradiation. Lower concentrations caused approximately 2 log reduction at maximum irradiation time. P123/Colalipid BP formulation containing THPP caused 1 to 3 log reduction in cell survival, depending on the PS and light dose. Applying PS solubilized in P123/Colalipid M formulation led to 1-2 log reduction after 30 min irradiation and a total eradication following 60 min irradiation. The PS dose did not significantly influence the cell survival. Figure 6 presents the treatment of CA2 strain with the three evaluated formulations at the selected light doses, compared to dark controls. While the cell survival did not change significantly following exposure to PS enriched formulations in dark, the light-irradiated cultures showed dose and light-dependent reduction in cell survival.

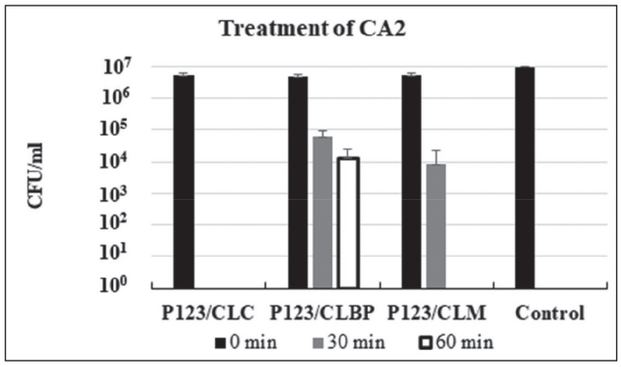

Fig. 6: Cell survival of *C. albicans* cells (CA2 strain) after aPDT treatment with 0,5 % P123/Colalipid C (P123/CLC), 0,5 % P123/Colalipid M (P123/CLM), 0,25 % P123/Colalipid BP (P123/CLBP) formulations containing 60 μM THPP (±SD; n=5).

3. Discussion

3.1. Photosensitizer solubilization

The absorption spectrum of THPP is highly dependent on solvent properties (Sobczyński et al. 2013). Due to its high lipophilicity (distribution coefficient, logD = 10.0 at pH 7) the PS is only slightly soluble in water, which is reflected by the flattened, broad Soret band in the aqueous environment (Fig. 2A). At neutral pH, THPP in aqueous solution is likely to be present in aggregated form. The porphyrin aggregation results in the PS stacking and formation of either horizontally displaced parallel planes of porphyrin, or stacked planes of porphyrin molecules. This results in the reduced lifetime of the excited PS triplet state due to a self-quenching effect, subsequently reducing $^1O_2$ production. Upon contact with P123 micelles, THPP will likely exhibit strong interactions with Pluronic copolymer possessing high average number of hydrophobic propylene oxide groups. As a result an efficient solubilization within the hydrophobic core of mixed micelles by P123/Colalipids assemblies is observed. This was demonstrated by the increase of THPP absorptivity and narrowing of the Soret band. The gradual red-shift of the absorption maximum has previously been associated with localization of THPP molecules within the core of the micelles (Sobczyński et al. 2013). At high concentration, P123/Colalipid BP assemblies yield better PS solubilization as compared to other P123/Colalipids assemblies. This is probably caused by higher hydrophobicity of the micellar core, provided by the presence of long C18 fatty acid chains of Colalipid BP. The results presented in Fig. 2B show that even 100x times dilution of the prepared formulation does not lead to a substantial reduction of the THPP absorptivity.

It is safe to assume, that during the photobiological experiments, THPP was solubilized by the prepared nanomicellar formulation even after mixing with the liquid growth medium. The present study had a limitation of including only low photosensitizer concentration (5 μM) in samples prepared for formulation characterization. Due to high PS absorptivity, the analysis of UV-Vis absorption spectra only yields valid results for low micromolar PS concentration range. At concentration exceeding ~ 7 μM the Soret band becomes high and wide, thus preventing solubilization analysis. However, the higher THPP concentrations, *i.e.* 60 μM were also efficiently solubilized, since no precipitation was observed in THPP samples at this concentration level. In this study the as lack of compound precipitation was evaluated by centrifugation of THPP solutions in order to detect a presence of undissolved compound within micellar formulations.

The process of Pluronic copolymer micellization comprises the arrangement of hydrophobic block within the micellar core and hydrophilic block on the outside, as micellar corona. Larger blocks with higher hydrophobicity arrange into micelles at lower copolymer concentrations. Short hydrophilic block result in higher aggregation number as more molecules are required to build the hydrophilic shell providing aqueous solubility. In binary surfactant systems composed incorporating surfactant molecules into Pluronic micelles eases micelle formation. The morphology of mixed micellar systems based on Colalipids and Pluronic P123 is highly dependent on the Colalipid chemical structure. The long unsaturated chains of borageamidopropyl moieties found in Colalipid BP are expected to be anchored in the hydrophobic micellar core together with propylene oxide block of Pluronic P123 stabilizing the micellar core. The charged PG-Dimonium groups are present in the hydrophilic micellar coronas together with ethylene oxide groups of Pluronic P123 increasing the hydrophilicity of the micellar corona. The charged groups found on the micelle surface are responsible for the positive charge found on the micellar outermost layer yielding highly positive zeta potential. Due to strong surface charge the P123/Colalipid BP assemblies are well soluble in water and micelles with low aggregation number are formed, as compared to uncharged pure Pluronic P123 micelles possessing only short hydrophilic blocks (Fig. 1). In P123/Colalipid BP formulation some larger micelles are also found, but the fraction comprising ~7 nm micelles is dominant. Since in photon correlation spectroscopy large particles yield stronger intensity signal, the real number of large micelles in this case is probably negligible.

Different situation is observed for the two systems formed by Colalipids C and M. These Colalipids are shorter molecules possessing C12-C14 and C14 chains for Colalipid C and Colalipid M, respectively. They are more deeply confined in the interior part of the micelle and their charged groups are probably accommodated closer to the micellar interface (palisade layer) and thus are less protruded into the exterior surface of the micellar coronas. Such arrangement results in lower zeta potentials and subsequent formation of larger micelles of 70 and 100 nm for the P123/Colalipid C and P123/Colalipid M assemblies, respectively. The inclusion of the hydrophobic solute has a substantial effect on the nanomicellar size. In case of all the evaluated P123/Colalipid assemblies the solubilization of the PS changes the bimodal size distribution into monomodal. Hydrophobic THPP molecules trapped within a core change the internal packing of the micellar core leading to its stabilization, probably by excluding water molecules bound to the copolymer chains. The preferential solubilization of THPP in the small micelle fraction is expected to be beneficial in regard to THPP delivery into fungal cells. The smaller nanoparticles exhibit higher surface to volume ration providing better opportunities for uptake by the targeted cells, as compared to their larger counterparts.

3.2. The in vitro photodynamic activity of nanocarrier formulations

Our previous investigations showed that P123 exhibits no antifungal activity (minimal fungicidal concentration, MFC > 1000 μg/ml; unpublished results). On the other hand, Colalipids exhibited low to high activity, depending on the molecule tested. The experimental MFC values were 62,5 μg/ml, 500 μg/ml and 1000 μg/ml

for Colalipid BP, Colalipid C and Colalipid M, respectively. It should be noted, however, that MFC assay includes long 16-20 hours incubation time, that is much longer as compared to the duration of photodynamic experiments performed in this study. In our case, P123/Colalipids assemblies proved ineffective to eradicate *C. albicans* on its own at concentration < 0,5% for P123/Colalipid C and P123/Colalipid M and at concentration < 0,25% for P123/Colalipid M. We thus decided to use the concentration that was non-toxic to fungal cells, but was high enough to disrupt their cell wall and ease intracellular PS delivery.

Cultures of *C. albicans* exposed to formulations containing THPP solubilized by P123/Colalipids assemblies, but not exposed to light irradiation were unharmed, as proved by our dark toxicity experiments. Cultures marked at Fig. 5 and 6 with '0 minutes' light exposure were kept in dark with the respective formulation for the whole duration of the experiment, *i.e.* 60 minutes, corresponding to the longest irradiation time. In order to elucidate the role of the nanomicellar formulation, photodynamic activity of THPP dissolved in DMSO was tested as well at 60 μM and 60 minutes irradiation time, showing no activity (data not shown). This was due to PS insolubility in the aqueous environment of the growth medium.

In our previous study, THPP was efficiently solubilized by pure P123 micelles (Sobczyński et al. 2015). In the present study, despite good solubility, the THPP-P123 assemblies showed no photobiological activity, nor any dark toxicity (data not shown). Only cultures exposed concomitantly to PS, P123/Colalipids and light were shown to reduce cell survival at the extent dependent on the type and concentration of these agents as well as the strain type. Our experiments showed that P123/Colalipid C formulations were the most effective in eradicating *C. albicans* cells, followed by P123/Colalipid M assemblies and P123/Colalipid BP formulations (Fig. 6). The photodynamic efficiency was inversely dependent on the nanoparticulate carrier's zeta potential. The formulation with the lowest surface charge was the most efficient. The positive charge surrounding the nanoparticles ensures columbic attraction to the negatively charged fungal cell surface. On the other hand, high surface charge renders nanoparticles highly hydrophilic. The hydrophilic character precludes strong interactions with phospholipids present in the fungal cell wall, effectively decreasing the active ingredient transport into the microbial cell membrane.

The second variable influencing the efficiency of the photodynamic treatment was the photosensitizer dose. While the increase in PS dose was shown to highly diminish the survival of *C. albicans* treated with THPP-P123/Colalipid C assemblies, the THPP-P123/Colalipid M and especially THPP-P123/Colalipid BP formulations proved to exhibit PS-independent effect. This further proves the significance of effective PS internalization provided by the nanocarrier. If the internalization is poor, only the PS molecules adhered to the cell surface can work, as the reactive oxygen species produced in the photochemical process exhibit only limited diffusion of ~20 nm (Agostinis et al. 2011). In such case the total PS dose applied to the culture dish does not matter, since only a fraction of PS molecules found in the vicinity of the fungal cells would contribute to the aPDT activity. On the contrary, the formulations that promote efficient cell internalization will provide a dose-dependent effect. In the latter case, the higher the total PS concentration is, the more molecules can be present at the active site.

Another factor influencing the photodynamic activity is the strain type. The clinical strain used in this study was shown to exhibit stronger lipolytic and weaker proteolytic activity as compared to model strain. The clinical isolate was susceptible to nystatin, amphotericin B, econazole and miconazole. In general, formulations exhibited stronger effect in *C. albicans* ATCC collection strain, as compared to clinically derived strain. The exception was the P123/Colalipid M formulation that showed a similar efficiency in both strains. It is known, that the hospital strains are generally less susceptible to treatment, as compared to model strain. The photosensitizer structure differs from commonly employed antifungal chemotherapeutics and cross-resistance is not expected. However, other drug-resistance mechanism, *e.g.* the presence of drug efflux pumps may be the reason for decreased efficiency of the THPP-P123/Colalipids formulation treatment of the CA2 strain. Even though the CA2 strain has proved a more difficult target for aPDT treatment, the treatment employing an optimized nanomicellar formulation caused a complete eradication of clinically relevant pathogens.

3.3. Conclusions

The influence of Pluronic P123/Colalipids nanomicellar formulations on solubilization, nanoparticle characteristics and *in vitro* photocytotoxicity in fungal cells was investigated. The P123/Colalipids assemblies efficiently solubilized and disaggregated porphyrin PS at nontoxic concentrations. While this effect was similar for all the evaluated formulations, the surface charge of the different P123/Colalipid combinations varied substantially. This further influenced the nanocarrier capacity to efficiently penetrate the biologic barrier of the *C. albicans* cell wall and to promote PS internalization into the fungal cell. Photodynamic efficiency of THPP *in vitro* was inversely proportional to the surface charge of the formulation, probably due to excessive hydrophilicity precluding strong interactions with the cell wall components. Concluding, Colalipids have been shown to be efficient modifiers of the P123 micelle properties. The THPP-P123 micellar system showed no photobiological activity, despite good THPP solubilization. However, the optimized formulations exhibited efficient aPDT activity towards both model and clinically relevant *C. albicans* strains. The results are promising in regard to further aPDT formulation based on mixed micellar nanocarriers.

4. Experimental

4.1. Materials

5,10,15,20-Tetrakis(4-hydroxyphenyl) porphine (THPP) was purchased from FrontierScientific, Logan, USA and used as received. Pluronic P123, was purchased from Sigma Aldrich (St. Louis, MO). Colalipid C (ocamidopropyl PG-Dimonium Chloride Phosphate), Colalipid M (Myristamidopropyl PG-Dimonium Chloride Phosphate) and Colalipid BP (Sodium Borageamidopropyl PG-Dimonium Chloride Phosphate) were gifts from Colonial Chemicals. The compounds were stored desiccated at + 4°C. Double distilled sterile water was used for all experiments. The Zeta potential transfer standard (-68±6.8 mV) and DipCell electrode assembly were purchased from Malvern Instruments Ltd. (Malvern, UK).

4.2. Sample preparations

Photosensitizer containing samples and blank samples (P123-Colalipid formulation without THPP as well as P123 dispersion) were prepared by solvent evaporation. Appropriate volumes of THPP stock solution (1 mg/ml), Pluronic P123 stock solution (0,1 g/ml) and Colalipids (0,05 g/ml) in methanol were mixed in a round bottle (100 ml). The methanol was evaporated (IKA RV8 rotary evaporator, IKA, Germany, 30 rpm) at 60±1°C during light protection and THPP-P123-Colalipid mixtures formed a film. Double distilled water (50 ml) was immediately added to the round bottle and the film was dissolved by agitation (125 rpm, SK-L330-PRO, D-lab) for 30 min at 25±1°C. All the samples were filtered using sterile nylon filters 0.45 μm), protected from light and allowed to equilibrate for 30 min at 25°C±1°C, prior to being used in further experiments.

4.3. UV-visible absorption measurements

The blank samples were diluted with double distilled water and enriched with an aliquot of THPP standard solution (1 mg/ml) and shaken for 30 min (125 rpm, SK-L330-PRO, D-lab). The methanol concentration in in the aqueous solutions never exceeded 2% (v/v) of the sample. UV-visible absorption spectra of THPP (5 μM) were recorded at various concentration of P123/Colalipid assembly. The accuracy in wavelength determination of the instrumentation was±0.5 nm. Samples were wrapped in aluminum foil prior to use in order to protect from light exposure. All spectra were recorded at 25°C (controlled by Peltier regulator).

4.4. Determination of particle size and zeta potential

Blank samples and samples containing P123 and Colalipids and THPP were prepared, as described earlier (Sample preparations). An aliquot of sample was transferred to a plastic cuvette (0.75 ml into a sizing cuvette or 70 μl into a microcuvette for z-potential or particle size measurements, respectively). Sample processing was done at 25±1 °C. The particle size and ζ-potential were determined by use of a Zetasizer (Malvern Nanosizer ZS, Malvern Instruments, UK), equipped with 633 nm laser, at 25±0.1 °C. Lower detection limit is 0.3 nm for particle size measurements, lower particle diameter is 3.8 nm for zeta potential measurements. Samples were equili-

brated for 120 s before each measurement (n=5). Automatic attenuation was used. The refractive index of polystyrene particles (1.59) was selected. Water was selected as a theoretical dispersant. The instrument was tested using the zeta potential standard prior to measurements. Quality of data was determined by assessing count rate and attenuation level.

4.4. Photobiological experiments

Two strains of *Candida albicans* were used in this study, model ATCC 10231 strain and clinical *C. albicans* isolated from a patient suffering from lung cancer patient hospitalized at cardiothoracic surgery ward in the Independent Public Clinical Hospital No. 4 in Lublin. The strains were stored at -20 °C in 50% glycerol and then cultured on Sabouraud dextrose agar with chloramphenicol at 30 ºC for 48 h. After the incubation period fresh colonies of fungi were subcultured on Sabouraud dextrose broth at 30 ºC for 48 h. Liquid fresh yeast culture (5 ml) was placed in a Petri dish and 5 ml of blank or THPP enriched formulation was added to the dish and mixed thoroughly by pipette. Following 15 min incubation time the dishes were kept in the dark, covered with aluminum foil (dark control) or exposed to blue light irradiation for a 10, 20, 30 or 60 min. Irradiation process was carried out by using Megalight ST lamp emitting blue light (420-450 nm) equipped with ORE-4 blue light bulbs (60 W power). Then 5 mL of the mixture were taken from the dish and an aliquot was plated automatically on Sabouraud dextrose agar with chloramphenicol using serial dilution mode by use of Easy Spiral Dilute (Interscience). During the process a 2log dilution was performed by the plater (double 10x times dilution). Petri dishes were aerobically incubated at 35 °C for 48 h. Then, colonies of *Candida albicans* were automatically counted on each plate using Scan 1200 colony counter (Intersciene) including the dilution previously performed by the plater. The results were presented as colony-forming units per milliliter (CFU/ml). All assays were carried out in three replicates, unless otherwise stated. As a control, the liquid culture of reference and clinical *C. albicans* strains with no added PS or excipient were used.

Acknowledgements: We would like to acknowledge Colonial Chemicals for free samples of Colalipids. This work was kindly supported by the National Science Centre grant No. 2015/17/D/NZ7/02171

Conflicts of interest: None declared.

References

Agostinis P, Berg K, Cengel KA, Foster TH, Girotti AW, Gollnick SO, Hahn SM, Hamblin MR, Juzeniene A, Kessel D, Korbelik M, Moan J, Mróz P, Nowis D, Piette J, Wilson BC, Gołąb J (2011) Photodynamic therapy of cancer: an update. CA Cancer J Clin 61: 250–281.

Batrakova EV, Kabanov AV (2008) Pluronic block copolymers: Evolution of drug delivery concept from inert nanocarriers to biological response modifiers, J Control Release 130: 98–106.

Beirão S, Fernandes S, Coelho J, Faustino MA, Tomé JP, Neves MGPMS, Tomé AC, Almeida A, Cunha A (2014) Photodynamic inactivation of bacterial and yeast biofilms with a cationic porphyrin. Photochem Photobiol 90: 1387–1396.

Dai T, Huang YY, Hamblin MR (2009) Photodynamic therapy for localized infections - State of the art. Photodiagn Photodyn 6: 170–188.

Devrim B, Bozkır A (2017) Nanocarriers and Their Potential Application as Antimicrobial Drug Delivery. In: Grumezescu AM (ed.) Nanostructures for Antimicrobial Therapy, Amsterdam, pp. 169-202.

Fost DL, Yablonski JI (1997) Biomimetic Phospholipids: Components for Self-Preservation. In: Kabara JJ, Orth DS (eds.) Preservative-Free and Self-Preserving Cosmetics and Drugs: Principles and Practice, New York, p. 139-158

Ghosh S, Carter KA, Lovell JF (2019) Liposomal formulations of photosensitizers. Biomaterials 218: 1–15.

Gouterman M (1978) Optical spectra and electronic structure of porphyrins and related rings. In: Dolphin d (ed.) Porphyrins, Volume III, Cambridge, pp. 1-165.

Hamblin MR, Hasan T (2004) Photodynamic therapy: a new antimicrobial approach to infectious disease? Photochem Photobiol Sci 3: 436e450.

Johnson GA, Ellis EA, Kim H, Muthukrishnan N, Snavely T, Pellois JP (2014) Photoinduced membrane damage of *E. coli* and *S. aureus* by the photosensitizer-antimicrobial peptide conjugate eosin-$(KLAKLAK)_2$. PLoS One 9: e91220.

King MJ, Badea I, Solomon J, Kumar P, Gaspar KJ, Foldvari M (2002) Transdermal delivery of insulin from a novel biphasic lipid system in diabetic rats. Diabetes Technol Ther 4: 479–488.

Lilletvedt M, Tønnesen HH, Høgset A, Sande SA, Kristensen S (2011a) Evaluation of physicochemical properties and aggregation of the photosensitizers TPCS2a and TPPS2a in aqueous media. Pharmazie 66: 325–333.

Lilletvedt M, Smistad G, Tønnesen HH, Høgset A, Kristensen S (2011b) Solubilization of the novel anionic amphiphilic photosensitizer TPCS2a by nonionic Pluronic block copolymers. Eur J Pharm Sci 43: 180–187.

Otto A, Wiechers JW, Kelly CL, Dederen, JC, Hadgraft J, Du Plessis J (2010) Effect of emulsifiers and their liquid crystalline structures in emulsions on dermal and transdermal delivery of hydroquinone, salicylic acid and octadecenedioic acid. Skin Pharmacol Phys 23: 273-282.

Paszko E, Ehrhardt C, Senge MO, Kelleher DP, Reynolds JV (2011) Nanodrug applications in photodynamic therapy. Photodiagn Photodyn Ther 8:14-29.

Pitto-Barry A, Barry NP (2014) Pluronic® block-copolymers in medicine: from chemical and biological versatility to rationalisation and clinical advances. Polym Chem 5: 3291-3297.

Sobczyński J, Tønnesen, HH, Kristensen, S (2013) Influence of aqueous media properties on aggregation and solubility of four structurally related meso-porphyrin photosensitizers evaluated by spectrophotometric measurements. Die Pharmazie 68: 100-109.

Sobczyński J, Kristensen S, Berg K (2014) The influence of Pluronics nanovehicles on dark cytotoxicity, photocytotoxicity and localization of four model photosensitizers in cancer cells. Photochem Photobiol Sci 13: 8-22.

Sobczyński J, Smistad G, Hegge AB, Kristensen S (2015) Molecular interactions and solubilization of structurally related meso-porphyrin photosensitizers by amphiphilic block copolymers (Pluronics). Drug Dev Ind Pharm 41:1237-1246.

Sobczyński J, Polski A (2017) Nanocarriers for Photosensitizers for Use in Antimicrobial Photodynamic Therapy. In: Grumezescu AM (ed.) Nanostructures for Antimicrobial Therapy, Amsterdam, pp. 481-502.

Sobczyński J, Chudzik-Rząd B (2018) Mixed micelles as drug delivery nanocarriers. In: Grumezescu AM (ed.) Design and Development of New Nanocarriers, Norwich, pp. 331–364.

Takasaki AA., Aoki A, Mizutani K, Schwarz F, Sculean A, Wang CY, Koshy G, Romanos G, Ishikawa I, Izumi Y (2009) Application of antimicrobial photodynamic therapy in periodontal and peri-implant diseases. Periodontology 51: 109–140.

Wainwright M (2009) Porphyrins. In: Wainwright M (ed.) Photosensitisers in Biomedicine, New Jersey, p. 113–146.